JOURNAL OF THEORETICAL AND APPLIED MECHANICS
60, 4, pp. 603-617, Warsaw 2022
https://doi.org/10.15632/jtam-pl/153002

MEMBRANE VERSUS BENDING COMPONENTS OF TRANSVERSE FORCES IN CYLINDRICAL PANELS IN THE CST AND THE FSDT

Zbigniew Kolakowski, Jacek Jankowski
Lodz University of Technology, Department of Strength of Materials, Lodz, Poland
e-mail: zbigniew.kolakowski@p.lodz.pl; jacek.jankowski@p.lodz.pl

A nonlinear problem of deflection of isotropic cylindrical panels fixed along all edges and subject to transverse load was considered within the first-order shear deformation theory (FSDT) and the classical shell theory (CST). An effect of the parameter of curvature on bending and membrane components and resultants of transverse forces was analyzed. Particular attention was drawn to the fact that the bending components were accompanied by transverse deformations, whereas for the membrane components, the panel was transversely perfectly rigid. Resultants of transverse forces can be significantly larger than the bending components. In failure criteria of laminated structures, only the bending transverse forces are employed.

Keywords: square cylindrical panels, nonlinear theories of panel structures, CST, FSDT, transverse shear forces

1. Introduction

More than 75 years ago Reissner (1944, 1945) proposed to extend Timoshenko's linear beam theory covering the transverse shear effect into a stress-based plate theory. A few years later Mindlin suggested to develop it into a theory based on the displacement approach (Mindlin, 1951). Hence, these two proposals have been referred to under a common name of the first-order shear deformation theory (FSDT) or the Reissner-Mindlin plate theory.

Higher-order shear theories were discussed in (Reddy, 2002, 2011). In (Reddy, 2011), a general third-order shear plate theory covering geometrical nonlinearities was presented for FGM plates. Simplifications in this theory, which has 11 generalized displacements compared to 5 displacements in the Reddy third-order theory through the first-order plate theory (FSDT) and the classical plate theory (CPT) with 3 displacements, were discussed. The Reissner boundary effect, which requires a rotational potential to be introduced for a fast-variable solution to the boundary layer, was presented in (Taylor *et al.*, 1997; Vasiliev, 2000; Vasiliev and Lurie, 1992). In (Cai *et al.*, 2002), a mixed finite element based on the mechanism of the shear locking phenomenon was analyzed. In the FEM, a problem of shear locking in the boundary layer occurs, as the shape functions cannot approximate a fast-variable solution to the boundary layer (Cen and Shang, 2015; Bathe, 1996). Within the FSDT, other variants are developed as well, e.g.: a two-variable refined plate theory (Endo and Kimura, 2007; Kim *et al.*, 2009; Park and Choi, 2018; Shimpi and Patel, 2006) and a single-variable refined theory (Shimpi *et al.*, 2017).

In (Kolakowski and Jankowski, 2020, 2021), the effect of bending and membrane components of transverse forces on total transverse forces within three nonlinear plate theories, namely: the CPT (classical plate theory), the S-FSDT (simple first-order shear deformation theory) and the FSDT for plate elements, was presented. Bending components of forces depend on derivatives of moments, which are accompanied by transverse deformations. Membrane components depend on projections of membrane forces on the transverse direction and do not affect transverse

deformations (Kolakowski and Jankowski, 2021). Bending components are linearly dependent on plate deflections, whereas membrane components – nonlinearly. Membrane components play an increasingly significant role along with an increase in deflections above half the plate thickness. Hence, it is necessary to account for nonlinear theories for finite plate deflections. A more comprehensive literature survey is given in (Kolakowski and Jankowski, 2020, 2021).

In this paper, the considerations discussed in (Kolakowski and Jankowski, 2021) referring to components of transverse forces within the nonlinear FSDT and CST (classical shell theory) (Volmir, 1967), but for square cylindrical steel panels of various curvatures fixed along all edges and subject to transverse load, are continued. Here, only fundamental equations and their solutions to the nonlinear problem of deflection of the square panel within the CST and the FSDT, where the Reissner boundary effect is neglected, are presented (Kolakowski and Jankowski, 2020, 2021).

2. Formulation of the problem

An analysis of the nonlinear problem of components of inner transverse forces in a thin-walled cylindrical panel of various parameters of curvature and subject to the transverse load q (Fig. 1) is discussed. The problem was solved for a square isotropic panel fixed along the whole perimeter within the FSDT and the CST. The panel material was assumed to obey Hooke's law.

Particular attention was paid to bending and membrane components and resultants of transverse forces for cylindrical panels. According to the two accepted theories, bending components for cylindrical panels are expressed with identical formulas as for the plate (Kolakowski and Jankowski, 2020, 2021). In contrast, membrane components for both theories are identical, with additional two components appearing for each curvature-induced component relative to the plate theory (see Appendix 2 for a more detailed analysis). Thus, attention was drawn to the influence of the panel curvature parameter k on components and resultants of transverse forces in the present work.

The appendix contains only the equations necessary to facilitate the readability of the paper (Appendix 1). A solution for a square isotropic panel was also given, with particular emphasis on membrane and bending components and resultants of transverse forces (Appendix 2).

The bending components are expressed with formulas (A.10) – FSDT, (A.16) – CST, respectively, which depend on the derivatives of inner moments in the plate. In the second term at the torsional moment for the FSDT, there is a factor equal to 1, and for the CST – this factor equals 2. The membrane components of (A.11) – FSDT and (A.17) – CST depend respectively on the projections of membrane forces on the direction perpendicular to the middle surface of the panel.

In the nonlinear theories, there are two nonlinear equations to solve the problem of nonlinear stability of thin plates. One of them is an equation of inseparability of deformations (A.7) depending on a function of the forces F and the deflection w. The second equation is an equation of equilibrium of projections of inner transverse forces on the perpendicular direction, including the transverse load q, which is written in an abbreviated form for the two theories considered according to (A.13) and (A.19) (see the Appendix) as

$$\int_0^l \int_0^b \Big[(\widehat{Q}^{\Theta}_{x,x} + \widehat{Q}^{\Theta}_{y,y}) + (\overline{Q}^{\Theta}_{x,x} + \overline{Q}^{\Theta}_{y,y}) + q^{\Theta} + \frac{N_y}{R} \Big] \delta w \, dx \, dy = 0 \tag{2.1}$$

here the upper index $\Theta = F, C$ denotes the FSDT, CST, correspondingly.

In the first round bracket in (2.1), there are linear bending components of transverse forces, and in the second bracket – nonlinear membrane components.

Comparing (A.10) and (A.16) for bending components, it can be seen that the components for the CST are larger than those for the FSDT. It should be remembered that expressions for the component moments are, however, different. According to (A.17), the corresponding membrane components of transverse forces $\overline{Q}_x^{\Theta}$, $\overline{Q}_y^{\Theta}$ in (2.1) for the theories under consideration are identical, because they depend only on the variables F, w in (2.1). These components do not affect transverse deformations.

Considering dependencies (A.12) and (A.18) in (2.1), we have

$$\int_0^l \int_0^b \Big(\widetilde{Q}_{x,x}^{\Theta} + \widetilde{Q}_{y,y}^{\Theta} + q^{\Theta} + \frac{N_y}{R} \Big) \delta w \, dx \, dy = 0 \tag{2.2}$$

In the above equation, in comparison to the plate theory (i.e., for $R = 0$), there is an additional last term associated with the membrane force in the direction of the panel arch, i.e., the y axis (Fig. 1).

Equation (2.1) for the CST, after consideration of (A.8), leads to one of the von Kármán equations

$$\begin{aligned} \int_0^l \int_0^b \Big[D(w_{,xxxx} + 2w_{,xxyy} + w_{,yyyy}) - \Big(F_{,yy} w_{,xx} - 2F_{,xy} w_{,xy} \\ + F_{,xx} w_{,yy} + \frac{F_{,xx}}{R} + q \Big) \Big] \delta w \, dx \, dy = 0 \end{aligned} \tag{2.3}$$

and the second equation is an equation of inseparability of deformations (A.7).

3. Analysis of the calculation results

A detailed analysis was carried out for a square steel panel (Fig. 1), similarly to square plates in (Kolakowski and Jankowski, 2020, 2021), with the following geometric dimensions and material constants

$$a = 150\,\text{mm} \qquad h = 1\,\text{mm} \qquad E = 200\,\text{GPa} \qquad \nu = 0.3$$

for five different values of the parameter of curvature $k = a^2/(Rh)$, where R is the radius of curvature of the cylindrical panel.

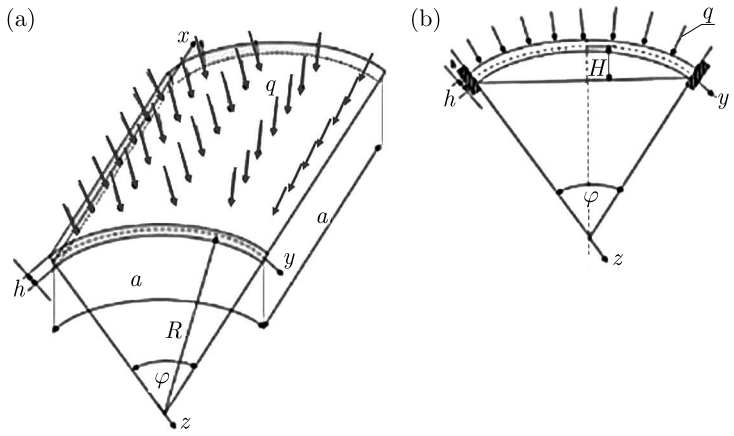

Fig. 1. Cylindrical square panel loaded transversely

The perfect plate is fixed along all edges and subject to the transverse load q. The boundary conditions for the theories under consideration are given in detail in Appendix 2.

The nonlinear equilibrium equations for both theories (A.25) and (A.31) can be written together as

$$\frac{533\pi^4}{3200}\zeta^3 + \frac{2\pi^4}{3(1-\nu^2)}\alpha^{\Theta}\zeta - \frac{15\pi^2}{64}k\zeta^2 + \frac{9}{64}k^2\zeta - \overline{q}^{\Theta} = 0 \tag{3.1}$$

where: $\overline{q}^{\Theta} = q^{\Theta}a^4/(Eh^4)$, $\zeta = W/h$, α^{Θ} are values of the reduction factor.

In detailed calculations, five values of the parameter of curvature were assumed, i.e., $k = 0$, 12, 24, 36, 48. For $k = 0$, the panel becomes a plate. According to (Volmir, 1967) for small angles Θ (Fig. 1), i.e., low values of the parameter of curvature k (i.e. for $0 \leqslant k \leqslant 12$), this parameter can be also determined from the approximate relationship $k = 8H/h$ (Fig. 1b).

In Fig. 2, a dependence of the transverse load $\overline{q}^C$ on the dimensionless deflection ζ for the assumed 5 values of the coefficient of curvature k is presented for the CST. The curve $k = 12$ coincides with the curve $k = 0$ (i.e., for a square plate) up to the deflection $\zeta \leqslant 1$, whereas the curves $k = 24$, $k = 36$ and $k = 48$ lie above the curve $k = 0$. This means that for $\zeta \leqslant 1$, the panel carries a greater load $\overline{q}^C$ than the plate, except for the panels for $k = 12$. For $\zeta \leqslant 1.7$, the curves for $k = 12$ and $k = 24$ lie below $k = 0$. In turn, for $\zeta \leqslant 2.2$ only the curve $k = 48$ lies above $k = 0$, and for $\zeta \approx 3$, the curves intersect. This results in a selection of two deflection values: $\zeta = 1$ and $\zeta = 2$ in order to determine components and resultants of transverse forces. For the first of these values, the power exponent in transverse forces (A.27), (A.28) and (A.33) does not play any role.

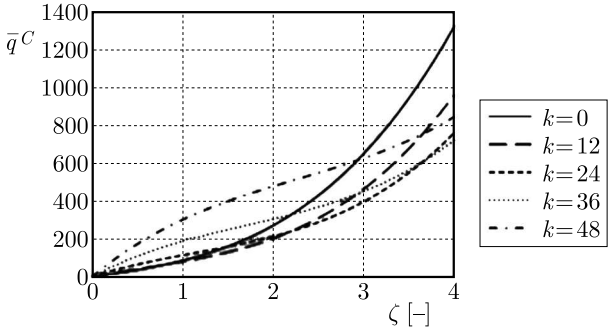

Fig. 2. Dependence of the transverse load $\overline{q}^C$ on the dimensionless deflection ζ

Tables 1 and 2 present the results of calculations according to the CST and the FSDT for the assumed dimensionless deflections $\zeta = 1.0$ and $\zeta = 2.0$ and the adopted parameters of curvature k. For the fixed deflection and the curvature parameter, the values of transverse loads q^C, q^F, the maximal absolute values of bending components $|\widehat{Q_x^C}|_{max}$, $|\widehat{Q_y^C}|_{max}$, membrane components $|\overline{Q_x^C}|_{max}$, $|\overline{Q_y^C}|_{max}$ and total components $|\widetilde{Q_x^C}|_{max}$, $|\widetilde{Q_y^C}|_{max}$ of transverse forces were determined for the CST. For the FSDT, the value of the reduction coefficient α and only the maximal absolute values of total transverse forces $|\widetilde{Q_x^F}|_{max}$ and $|\widetilde{Q_y^F}|_{max}$ were given. Membrane components (A.34), according to the CST and the FSDT, are identical (see also (Kolakowski and Jankowski, 2020, 2021).

As can be easily seen in Table 1, the transverse load q^C for $k = 24$ is almost 1.3 times greater than for $k = 0$, 2.1 times greater for $k = 36$ and 3.4 times greater for $k = 48$, respectively. The values of bending components (A.27) $|\widehat{Q_x^C}|_{max}$, $|\widehat{Q_y^C}|_{max}$ for the CST do not depend on the parameter k. An identical situation takes place for (A.33) $|\widehat{Q_x^F}|_{max}$, $|\widehat{Q_y^F}|_{max}$ in the FSDT. Membrane components (A.28), (A.34) for both the theories are identical (i.e., $|\underline{Q_x^C}|_{max} = |\overline{Q_x^F}|_{max}$, $|\overline{Q_y^C}|_{max} = |\overline{Q_y^F}|_{max}$), but are dependent on the parameter k. That means

Table 1. Values of loads of the square plate and absolute maximal values of the components and total transverse forces for $\zeta = 1.0$

Theory	Symbol	Unit	k				
			0	12	24	36	48
CST	α^C	–	1.0				
	q^C	MPa	0.0346	0.0316	0.0447	0.0737	0.1187
	$\lvert\widetilde{Q_x^C}\rvert_{max}$	N/mm	1.245	1.245	1.245	1.245	1.245
	$\lvert\widetilde{Q_y^C}\rvert_{max}$	N/mm	1.245	1.245	1.245	1.245	1.245
	$\lvert\overline{Q_x^C}\rvert_{max}$	N/mm	0.313	0.278	0.304	0.360	0.423
	$\lvert\overline{Q_y^C}\rvert_{max}$	N/mm	0.313	0.281	0.848	1.421	1.996
	$\lvert\widehat{Q_x^C}\rvert_{max}$	N/mm	1.530	1.523	1.528	1.546	1.574
	$\lvert\widehat{Q_y^C}\rvert_{max}$	N/mm	1.530	0.965	0.607	0.631	0.798
	$\lvert\overline{Q_x^C}\rvert_{max}/\lvert\widetilde{Q_x^C}\rvert_{max}$	–	0.21	0.18	0.20	0.23	0.27
	$\lvert\overline{Q_y^C}\rvert_{max}/\lvert\widetilde{Q_y^C}\rvert_{max}$	–	0.21	0.29	1.40	2.25	2.50
FSDT	α^F	–	0.9995				
	q^F	MPa	0.0346	0.0316	0.0447	0.0737	0.1187
	$\lvert\widetilde{Q_x^F}\rvert_{max}$	N/mm	1.296	1.287	1.293	1.314	1.346
	$\lvert\widetilde{Q_y^F}\rvert_{max}$	N/mm	1.296	0.729	0.552	0.631	1.019
	$\lvert\overline{Q_x^F}\rvert_{max}/\lvert\widetilde{Q_x^F}\rvert_{max}$	–	0.24	0.22	0.24	0.27	0.31
	$\lvert\overline{Q_y^F}\rvert_{max}/\lvert\widetilde{Q_y^F}\rvert_{max}$	–	0.24	0.39	1.54	2.25	1.96

Table 2. Values of loads of the square plate and absolute maximal values of the components and total transverse forces for $\zeta = 2.0$

Theory	Symbol	Unit	k				
			0	12	24	36	48
CST	α^C	–	1.0				
	q^C	MPa	0.108	0.080	0.084	0.120	0.188
	$\lvert whQ_x^C\rvert_{max}$	N/mm	2.49	2.49	2.49	2.49	2.49
	$\lvert\widehat{Q_y^C}\rvert_{max}$	N/mm	2.49	2.49	2.49	2.49	2.49
	$\lvert\overline{Q_x^C}\rvert_{max}$	N/mm	2.50	2.32	2.23	2.27	2.44
	$\lvert\overline{Q_y^C}\rvert_{max}$	N/mm	2.50	0.81	2.25	4.50	6.79
	$\lvert\widehat{Q_x^C}\rvert_{max}$	N/mm	4.87	4.76	4.71	4.74	4.82
	$\lvert\widehat{Q_y^C}\rvert_{max}$	N/mm	4.87	2.56	1.75	2.15	4.33
	$\lvert\overline{Q_x^C}\rvert_{max}/\lvert\widehat{Q_x^C}\rvert_{max}$	–	0.51	0.49	0.47	0.48	0.51
	$\lvert\overline{Q_y^C}\rvert_{max}/\lvert\widehat{Q_y^C}\rvert_{max}$	–	0.51	0.32	1.29	2.09	1.57
FSDT	α^F	–	0.9995				
	q^F	MPa	0.108	0.080	0.084	0.120	0.188
	$\lvert\widehat{Q_x^F}\rvert_{max}$	N/mm	4.41	4.29	4.24	4.27	4.36
	$\lvert\widehat{Q_y^F}\rvert_{max}$	N/mm	4.41	2.12	1.74	2.50	4.79
	$\lvert\overline{Q_x^F}\rvert_{max}/\lvert\widehat{Q_x^F}\rvert_{max}$	–	0.57	0.54	0.53	0.53	0.56
	$\lvert\overline{Q_y^F}\rvert_{max}/\lvert\widehat{Q_y^F}\rvert_{max}$	–	0.57	0.38	1.29	1.80	1.42

that the resultant transverse forces $|\widetilde{Q_x^C}|_{max}$, $|\widetilde{Q_y^C}|_{max}$ depend on the value of k. Moreover, the ratios $|\overline{Q_x^\Theta}|_{max}/|\widetilde{Q_x^\Theta}|_{max}$, $|\overline{Q_y^\Theta}|_{max}/|\widetilde{Q_y^\Theta}|_{max}$ (where $\Theta = C$ for the CST and F for the FSDT) are given.

In order to improve the readability, the results from Tables 1 and 2 are shown in the figures: for $\zeta = 1.0$ in Figs. 3-4 and $\zeta = 2.0$ in Figs. 5-6, correspondingly.

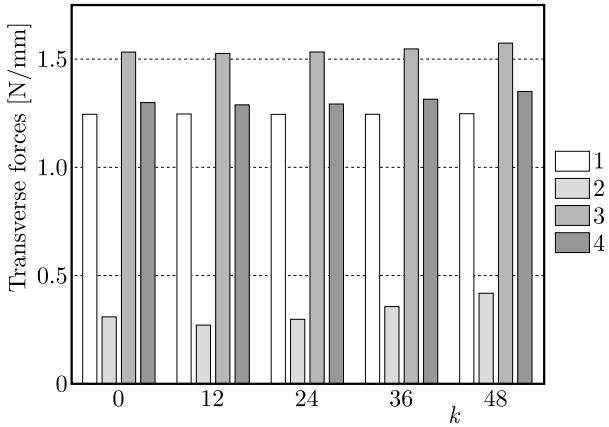

Fig. 3. Transverse forces: (1) – $|\widehat{Q_x^C}|_{max}$, (2) – $|\overline{Q_x^C}|_{max}$, (3) – $|\widetilde{Q_x^C}|_{max}$, (4) – $|\widetilde{Q_x^F}|_{max}$ as a function of the parameter of curvature k for $\zeta = 1.0$

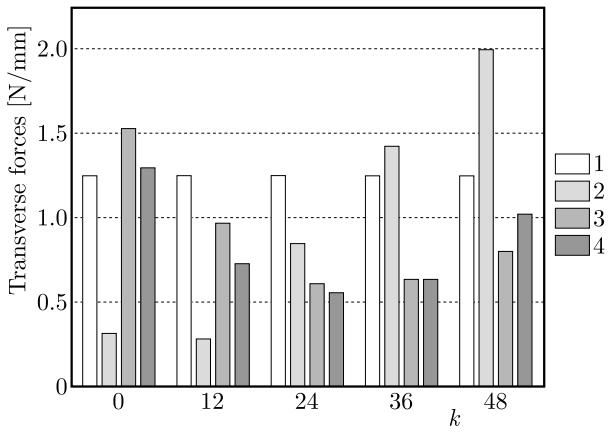

Fig. 4. Transverse forces: (1) – $|\widehat{Q_y^C}|_{max}$, (2) – $|\overline{Q_y^C}|_{max}$, (3) – $|\widetilde{Q_y^C}|_{max}$, (4) – $|\widetilde{Q_y^F}|_{max}$ as a function of the parameter of curvature k for $\zeta = 1.0$

As can be easily seen for $\zeta = 1.0$ in Fig. 3, the component $|\widehat{Q_x^C}|_{max}$ for all k is more than 3 times higher than $|\overline{Q_x^C}|_{max}$. Moreover, the component $|\widetilde{Q_x^C}|_{max}$ is higher than the bending components and the resultant $|\widetilde{Q_x^F}|_{max}$. In Fig. 4, the components $|\widetilde{Q_x^C}|_{max} \geqslant |\overline{Q_y^C}|_{max}$ for $k \leqslant 24$ and the opposite relationships hold for higher values. For $k = 0$, the resultants $|\widetilde{Q_y^C}|_{max}$ and $|\widetilde{Q_y^F}|_{max}$ are the greatest among all values of k, and for $k \geqslant 12$, they are lower than the bending components $|\widehat{Q_y^C}|_{max}$.

In Fig. 5 for $\zeta = 2.0$, the bending components $|\widehat{Q_x^C}|_{max}$ do not depend on the parameter k, and, what is more, the following relationships hold: $|\widehat{Q_x^C}|_{max} \approx |\overline{Q_x^C}|_{max}$, $|\widetilde{Q_x^C}|_{max} > |\widetilde{Q_x^F}|_{max}$ and $2|\widehat{Q_x^C}|_{max} \approx |\widetilde{Q_x^C}|_{max}$. In Fig. 6, for $k = 0$, we have the relationships: $|\widehat{Q_y^C}|_{max} \approx |\overline{Q_y^C}|_{max}$ and $|\widetilde{Q_y^C}|_{max} > |\widetilde{Q_y^F}|_{max}$, as well as $2|\widehat{Q_y^C}|_{max} \approx |\widetilde{Q_x^C}|_{max}$. For $k = 12$, the membrane component $|\overline{Q_y^C}|_{max}$ is the lowest and it increases with an increase in k. For $k \geqslant 36$, we have $|\overline{Q_y^C}|_{max} > |\widetilde{Q_y^C}|_{max}$.

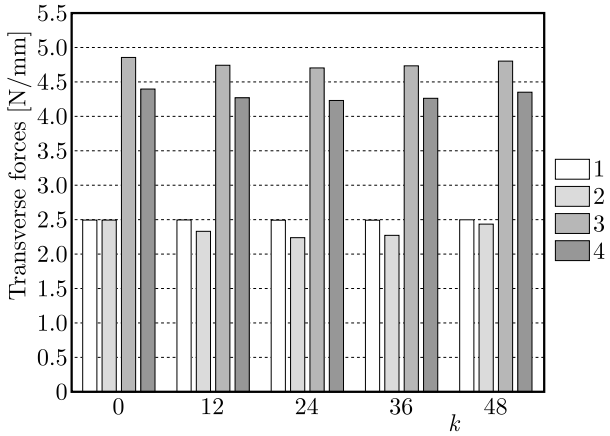

Fig. 5. Transverse forces: (1) – $|\widehat{Q_x^C}|_{max}$, (2) – $|\overline{Q_x^C}|_{max}$, (3) – $|\widetilde{Q_x^C}|_{max}$, (4) – $|\widetilde{Q_x^F}|_{max}$ as a function of the parameter of curvature k for $\zeta = 2.0$

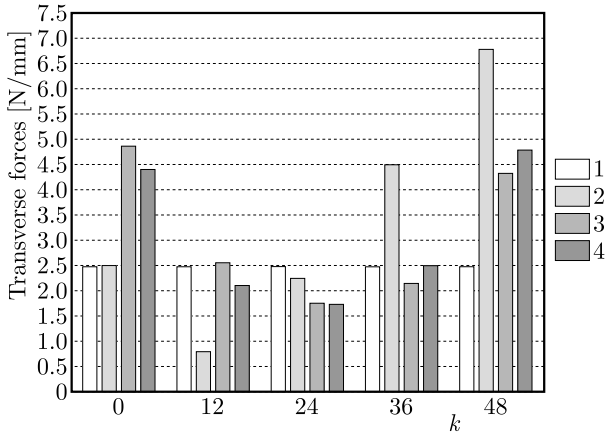

Fig. 6. Transverse forces: (1) – $|\widehat{Q_y^C}|_{max}$, (2) – $|\overline{Q_y^C}|_{max}$, (3) – $|\widetilde{Q_y^C}|_{max}$, (4) – $|\widetilde{Q_y^F}|_{max}$ as a function of the parameter of curvature k for $\zeta = 2.0$

Only for $k = 36$ and $k = 48$, we have $|\widetilde{Q_y^C}|_{max} \leqslant |\widetilde{Q_y^F}|_{max}$ (Figs. 4 and 6). In the remaining cases $|\widetilde{Q_\delta^C}|_{max} > |\widetilde{Q_\delta^F}|_{max}$, where $\delta = x, y$.

For $\zeta = 1.0$ and for all k, we have $2|\widehat{Q_x^C}|_{max} \approx |\widetilde{Q_x^C}|_{max}$ (see Fig. 3). Moreover, for $k = 0$ and $k = 36$, we have $1.2|\widehat{Q_y^C}|_{max} \approx |\widetilde{Q_y^C}|_{max}$, and for $k = 48$ – $1.6|\widehat{Q_y^C}|_{max} \approx |\widetilde{Q_y^C}|_{max}$, whereas for $k = 12$ and $k = 24$ – $|\widehat{Q_y^C}|_{max} > |\widetilde{Q_y^C}|_{max}$ (Fig. 4). For $\zeta = 2.0$, similarly as for $\zeta = 1.0$, $2|\widehat{Q_x^C}|_{max} \approx |\widetilde{Q_x^C}|_{max}$ holds (Fig. 5). For $k = 12$, $k = 24$, $k = 36$, we have $|\widehat{Q_y^C}|_{max} \approx |\widetilde{Q_y^C}|_{max}$, whereas for $k = 0$, 48 – $1.8|\widehat{Q_y^C}|_{max} \approx |\widetilde{Q_y^C}|_{max}$ (Fig. 6). This juxtaposition shows that the relations between bending components of transverse forces and resultants of transverse forces are complex for the panel (see (A.27), (A.28), (A.33) and (A.34)). Thus, in nonlinear problems, the resultants of transverse forces, which should be used in failure criteria for laminated structures, ought to be determined.

Tables 1 and 2 also give the ratios of membrane components to resultants of transverse forces $|\overline{Q_x^\Theta}|_{max}/|\widetilde{Q_x^\Theta}|_{max}$ and $|\overline{Q_y^\Theta}|_{max}/|\widetilde{Q_y^\Theta}|_{max}$ (where $\Theta = C$ for the CST and F for the FSDT). For $|\overline{Q_y^\Theta}|_{max}/|\widetilde{Q_y^\Theta}|_{max}$ and $k \geqslant 24$, the ratios are higher than 1. This means that the maximal absolute membrane components are greater than the maximal absolute bending components and have opposite signs.

4. Conclusions

Bending and membrane components and resultants of transverse forces for an isotropic square panel loaded transversely for different values of curvature within the framework of the nonlinear CST and FSDT have been analyzed. The bending components within the FSDT are accompanied by transverse deformations, whereas the cross-section is perfectly rigid for the membrane components. This shows the duality of assumptions within the FSDT. For the CST, cross-sections are non-deformable for the membrane and bending components of transverse forces.

Attention was drawn to the components and resultants of transverse forces for an isotropic cylindrical panel in order to show the influence of curvatures on their values on a simple example. According to the authors, in the case of laminated structures, the resultants of transverse forces should be considered in order to correctly describe the phenomenon of delamination.

Appendix

A1. Fundamental equations for cylindrical panels according to the FSDT and the CST

In (Reddy, 2004, 2011; Vasiliev, 2000; Vasiliev and Lurie, 1992; Endo and Kimura, 2007; Kim *et al.*, 2009; Park and Choi, 2018; Shimpi and Patel, 2006; Kolakowski and Jankowski, 2020, 2021; Volmir, 1972), the equations for three plate theories, namely: the first-order shear deformation plate theory (FSDT), the classical plate theory (CPT) and the simple first-order shear deformation theory (S-FSDT), were derived. The equilibrium equations and the boundary conditions were obtained within a variational approach.

This Appendix presents only the fundamental equations of the first two theories adopted to the theory of low-profile shells. The CPT for shells is referred to as Kirchhoff-Love's classical shell theory (CST).

The geometric relationships for the FSDT are assumed in the form (Reddy, 2004, 2011; Volmir, 1972)

$$\begin{aligned} &\varepsilon_x = u_{,x} + \frac{1}{2}w_{,x}^2 \qquad \varepsilon_y = v_{,y} + \frac{1}{2}w_{,y}^2 - \frac{w}{R} \\ &2\varepsilon_{xy} = \gamma_{xy} = u_{,y} + v_{,x} + w_{,x}w_{,y} \end{aligned} \tag{A.1}$$

and

$$\kappa_x = -\psi_{x,x} \qquad \kappa_y = -\psi_{y,y} \qquad \kappa_{xy} = -(\psi_{x,y} + \psi_{y,x}) \tag{A.2}$$

where: u, v, w are components of the plate displacement vector along the directions of the x, y, z axes, respectively, $\psi_x \psi_y$ – angles of rotation of the transverse normal with respect to bending around the x, y axis, respectively, xy – middle plane before buckling, R – radius of cylindrical panels. In addition, the following notations are introduced, e.g., $u_{,x} = \partial u/\partial x$.

In the FSDT for shells, the same as for plates, it is assumed that the total angles of rotation of the normal to the middle surface in two planes are (Kolakowski and Jankowski, 2020, 2021; Volmir, 1972)

$$w_{,x} = \psi_x + \beta_x \qquad w_{,y} = \psi_y + \beta_y \tag{A.3}$$

where β_x, β_y are transverse shear angles.

The inner cross-sectional forces can be expressed as (Kolakowski and Jankowski, 2020, 2021; Volmir, 1972)

$$N_x = \frac{Eh}{1-\nu^2}(\varepsilon_x + \nu\varepsilon_y) \qquad N_y = \frac{Eh}{1-\nu^2}(\varepsilon_y + \nu\varepsilon_x) \qquad N_{xy} = Gh\gamma_{xy} \tag{A.4}$$

$$M_x^F = -D(\psi_{x,x} + \nu\psi_{y,y}) \qquad M_y^F = -D(\psi_{y,y} + \nu\psi_{x,x})$$
$$M_{xy}^F = -D\frac{1-\nu}{2}(\psi_{x,y} + \psi_{y,x}) \tag{A.5}$$

$$\widehat{Q}_x^F = K^2Gh(w_{,x} - \psi_x) \qquad \widehat{Q}_y^F = K^2Gh(w_{,y} - \psi_y) \tag{A.6}$$

where K is the shear correction factor, and, moreover, the upper index F is introduced for the FSDT.

The system of equations (A.1) can be reduced to the equation of inseparability/continuity of deformations (Reddy, 2004, 2011; Kolakowski and Jankowski, 2021; Volmir, 1967)

$$\nabla\nabla F \equiv F_{,xxxx} + 2F_{,xxyy} + F_{,yyyy} = E\Big(w_{,xy}^2 - w_{,xx}w_{,xy} - \frac{w_{,xx}}{R}\Big) \tag{A.7}$$

where the Airy force function F was introduced

$$N_x = \sigma_x h = F_{,yy} \qquad N_y = \sigma_y h = F_{,xx} \qquad N_{xy} = \tau_{xy}h = -F_{,xy} \tag{A.8}$$

Equation (A.7) is linear with respect to F and nonlinear with respect to w.

A1.1. FSDT

According to the FSDT, the equilibrium equations for a cylindrical panel in variational terms are of the form (Kolakowski and Jankowski, 2020, 2021; Volmir, 1972)

$$\int_0^l\int_0^b (N_{x,x} + N_{xy,y})\delta u \; dx\, dy = 0 \qquad \int_0^l\int_0^b (N_{xy,x} + N_{y,y})\delta v \; dx\, dy = 0$$
$$\int_0^l\int_0^b \Big[\widehat{Q}_{x,x}^F + \widehat{Q}_{y,y}^F + \frac{N_y}{R} + (N_x w_{,x} + N_{xy}w_{,y})_{,x} + (N_{xy}w_{,x} + N_y w_{,y})_{,y} + q\Big]\delta w \; dx\, dy = 0 \tag{A.9}$$
$$\int_0^l\int_0^b (M_{x,x}^F + M_{xy,y}^F - \widehat{Q}_x^F)\delta\psi_x \; dx\, dy = 0$$
$$\int_0^l\int_0^b (M_{xy,x}^F + M_{y,y}^F - \widehat{Q}_y^F)\delta\psi_y \; dx\, dy = 0$$

The first two equations of equilibrium are identity-satisfied by the force function F (A.8).

The last two relationships in (A.9) give the bending components of transverse forces (Kolakowski and Jankowski, 2020, 2021)

$$\widehat{Q}_x^F = M_{x,x}^F + M_{xy,y}^F \qquad \widehat{Q}_y^F = M_{y,y}^F + M_{xy,x}^F \tag{A.10}$$

These components depend on the derivatives of inner bending moments (A.5). The transverse shear angles β_x, β_y in (A.3) correspond only to the bending components.

In turn, the membrane components of transverse forces were introduced, analogously to (Kolakowski and Jankowski, 2020, 2021)

$$\overline{Q}_x^F = N_x w_{,x} + N_{xy}w_{,y} \qquad \overline{Q}_y^F = N_y w_{,y} + N_{xy}w_{,x} \tag{A.11}$$

The membrane components of transverse forces depend on the projections of membrane forces on the transverse direction and do not affect membrane deformations. This means that the membrane components are not accompanied by deformations, unlike the bending components (Kolakowski and Jankowski, 2021).

In accordance with (A.10) and (A.11), a concept of resultants of total transverse forces $\widetilde{Q}_x^F$ and $\widetilde{Q}_y^F$ was introduced and defined as

$$\begin{aligned}\widetilde{Q}_x^F &= \widehat{Q}_x^F + \overline{Q}_x^F = (M_{x,x}^F + M_{xy,y}^F) + (N_x w_{,x} + N_{xy} w_{,y}) \\ \widetilde{Q}_y^F &= \widehat{Q}_y^F + \overline{Q}_y^F = (M_{y,y}^F + M_{xy,x}^F) + (N_y w_{,y} + N_{xy} w_{,x})\end{aligned} \tag{A.12}$$

Considering (A.12) in the third relationship (A.9), the following equilibrium equation is obtained

$$\int_0^l \int_0^b \Big[(\widehat{Q}_{x,x}^F + \widehat{Q}_{y,y}^F) + (\overline{Q}_{x,x}^F + \overline{Q}_{y,y}^F) + \frac{N_y}{R} + q\Big]\delta w \; dx\, dy = 0 \tag{A.13}$$

As can be easily seen, the terms corresponding to the membrane and bending derivatives of transverse forces, the circumferential force related to the radius and the transverse load q occur in the above equation.

It follows from relations (A.5) and (A.6) that the bending components of transverse forces $\widehat{Q}_x^F$ and $\widehat{Q}_y^F$ are linearly dependent on the variables ψ_x, ψ_y, w, whereas we have nonlinear relationships of the variables F, w from formulas (A.8), $(A.9)_3$ for the membrane components $\overline{Q}_x^F$ and $\overline{Q}_y^F$. Thus, equation (A.13) depends in the third power on w.

A1.2. CST

In the classical shell theory (i.e., Kirchhoff-Love's theory) in (A.3), it is assumed that $\beta_x = \beta_y = 0$ (i.e., $w_{,x} = \psi_x$, $w_{,y} = \psi_y$), and, moreover, the transverse forces are disregarded (A.6).

Considering the above for the CST in (A.5), we have

$$\begin{aligned}M_x^C &= -D(w_{,xx} + \nu w_{,yy}) \qquad & M_y^C &= -D(w_{,yy} + \nu w_{,xx}) \\ M_{xy}^C &= -D(1-\nu) w_{,xy}\end{aligned} \tag{A.14}$$

where the upper index C denotes the CST.

After considering the above-mentioned relationships, the equilibrium equation is of the form (Kolakowski and Jankowski, 2020, 2021; Volmir, 1967, 1972)

$$\begin{aligned}\int_0^l \int_0^b \Big[&M_{x,xx}^C + 2M_{xy,xy}^C + M_{y,yy}^C + (N_x w_{,x} + N_{xy} w_{,y})_{,x} \\ &+ (N_{xy} w_{,x} + N_y w_{,y})_{,y} + \frac{N_y}{R} + q\Big]\delta w \; dx\, dy = 0\end{aligned} \tag{A.15}$$

The second equation is an equation of inseparability (A.7).

The CPT defines Kirchhoff's substitutive transverse forces

$$\widehat{Q}_x^C = M_{x,x}^C + 2M_{xy,y}^C \qquad \widehat{Q}_y^C = M_{y,y}^C + 2M_{xy,x}^C \tag{A.16}$$

Identical to the FSDT, the membrane components of transverse forces are defined

$$\overline{Q}_x^C = \overline{Q}_x^F = N_x w_{,x} + N_{xy} w_{,y} \qquad \overline{Q}_y^C = \overline{Q}_y^F = N_y w_{,y} + N_{xy} w_{,x} \tag{A.17}$$

The above components of transverse forces are, therefore, membrane components of Kirchhoff's forces and have the same structure as for the FSDT. According to (A.16) and (A.17), Kirchhoff's total transverse forces $\widetilde{Q}_x^C$ and $\widetilde{Q}_y^C$ for the CPT are written as

$$\begin{aligned}\widetilde{Q}_x^C &= \widehat{Q}_x^C + \overline{Q}_x^C = (M_{x,x}^C + 2M_{xy,y}^C) + (N_x w_{,x} + N_{xy} w_{,y}) \\ \widetilde{Q}_y^C &= \widehat{Q}_y^C + \overline{Q}_y^C = (M_{y,y}^C + 2M_{xy,x}^C) + (N_y w_{,y} + N_{xy} w_{,x})\end{aligned} \tag{A.18}$$

Considering the above, equilibrium equation (A.15) finally takes the form

$$\int_0^l \int_0^b \Big[(\widehat{Q}^C_{x,x} + \widehat{Q}^C_{y,y}) + (\overline{Q}^C_{x,x} + \overline{Q}^C_{y,y}) + q + \frac{N_y}{R}\Big]\delta w \, dx \, dy = 0 \tag{A.19}$$

Similarly to the FSDT, the bending components of transverse forces $\widehat{Q}^C_x$ and $\widehat{Q}^C_y$ are linearly dependent on the variable w, whereas the membrane components $\overline{Q}^C_x$ and $\overline{Q}^C_y$ are nonlinearly dependent on the variables F, w. Comparing the formulas for the bending components of transverse forces (A.10) and (A.16), it can be seen that the numerical factor for the second term equals 1 for the FSDT, and it is 2 for the CST, respectively.

A2. Solution to the nonlinear problem of transverse distributions of shear forces in a square cylindrical panel subject to transverse load

In the work, a square isotropic cylindrical panel fixed along all edges and subject to the constant transverse load q (Fig. 1) is considered. It is assumed that the square panel with dimensions a, thickness h and radius R has the following material constants: Young's modulus E and Poisson's ratio ν. Considerations are limited to the elastic range. The problem has been solved within the first nonlinear approximation.

A2.1. Solution to the equation of inseparability of deformations

The equation of inseparability of deformations (A.7) is identical for both the theories under consideration: FSDT and CST.

The deflection of the square plate fixed along all edges within the first approximation is approximated with the following function (Kolakowski and Jankowski, 2021; Volmir, 1967, 1972)

$$w = W \sin^2 \frac{\pi x}{a} \sin^2 \frac{\pi y}{a} \tag{A.20}$$

which meets the following boundary conditions

$$\begin{aligned} &w(x=0) = w(x=a) = w(y=0) = w(y=a) = 0 \\ &w_{,x}(x=0) = w_{,x}(x=a) = w_{,y}(y=0) = w_{,y}(y=a) = 0 \end{aligned} \tag{A.21}$$

After substitution of (A.20) into (A.7), the Airy function F is determined

$$\begin{aligned} F = EhW^2\Big(&\frac{1}{32}\cos\frac{2\pi x}{a} + \frac{1}{32}\cos\frac{2\pi y}{a} - \frac{1}{512}\cos\frac{4\pi x}{a} - \frac{1}{512}\cos\frac{4\pi y}{a} \\ &+ \frac{1}{800}\cos\frac{4\pi x}{a}\cos\frac{2\pi y}{a} + \frac{1}{800}\cos\frac{2\pi x}{a}\cos\frac{4\pi y}{a} - \frac{1}{64}\cos\frac{2\pi x}{a}\cos\frac{2\pi y}{a}\Big) \\ &- \frac{EWha^2}{16\pi^2 R}\cos\frac{2\pi x}{a} + \frac{EWha^2}{64\pi^2 R}\cos\frac{2\pi x}{a}\cos\frac{2\pi y}{a} \end{aligned} \tag{A.22}$$

and then, according to (A.8), the components of membrane forces are determined

$$
\begin{aligned}
N_x &= F_{,yy} = EhW^2\Big(\frac{\pi}{a}\Big)^2\Big(-\frac{1}{8}\cos\frac{2\pi y}{a}+\frac{1}{32}\cos\frac{4\pi y}{a}-\frac{1}{200}\cos\frac{4\pi x}{a}\cos\frac{2\pi y}{a}\\
&\quad-\frac{1}{50}\cos\frac{2\pi x}{a}\cos\frac{4\pi y}{a}+\frac{1}{16}\cos\frac{2\pi x}{a}\cos\frac{2\pi y}{a}\Big)-\frac{EWh}{16R}\cos\frac{2\pi x}{a}\cos\frac{2\pi y}{a}\\
N_y &= F_{,xx} = EhW^2\Big(\frac{\pi}{a}\Big)^2\Big(-\frac{1}{8}\cos\frac{2\pi x}{a}+\frac{1}{32}\cos\frac{4\pi x}{a}-\frac{1}{50}\cos\frac{4\pi x}{a}\cos\frac{2\pi y}{a}\\
&\quad-\frac{1}{200}\cos\frac{2\pi x}{a}\cos\frac{4\pi y}{a}+\frac{1}{16}\cos\frac{2\pi x}{a}\cos\frac{2\pi y}{a}\Big)-\frac{EWh}{16R}\cos\frac{2\pi x}{a}\cos\frac{2\pi y}{a}\\
&\quad+\frac{EWh}{4R}\cos\frac{2\pi x}{a}\\
N_{xy} &= -F_{,xy} = -EhW^2\Big(\frac{\pi}{a}\Big)^2\Big(\frac{1}{100}\sin\frac{4\pi x}{a}\sin\frac{2\pi y}{a}+\frac{1}{100}\sin\frac{2\pi x}{a}\sin\frac{4\pi y}{a}\\
&\quad-\frac{1}{16}\sin\frac{2\pi x}{a}\sin\frac{2\pi y}{a}\Big)+\frac{EWh}{16R}\sin\frac{2\pi x}{a}\sin\frac{2\pi y}{a}
\end{aligned}
\tag{A.23}
$$

Force functions (A.23) satisfy the following boundary conditions (Kolakowski and Jankowski, 2021; Volmir, 1967)

$$
\begin{aligned}
&u(x=0)=u(x=a)=\text{ const} \qquad && N_{xy}(x=0)=N_{xy}(x=a)=0\\
&v(y=0)=v(y=a)=\text{ const} \qquad && N_{xy}(y=0)=N_{xy}(y=a)=0
\end{aligned}
\tag{A.24}
$$

.0.1. A2.2. Solution to the nonlinear stability problem for the CST

The nonlinear problem for the CST (A.15) or (A.19) with respect to w has been solved with the Bubnov-Galerkin method. After introduction of force function (A.23) and the deflection function w in (A.20), a nonlinear equilibrium equation of the square panel subject to the transverse load q for the CST (Kolakowski and Jankowski, 2021; Volmir, 1967) was obtained

$$
\frac{533\pi^4}{3200}\zeta^3+\frac{2\pi^4}{3(1-\nu^2)}\zeta-\frac{15\pi^2}{64}k\zeta^2+\frac{9}{64}k^2\zeta-q^C=0 \tag{A.25}
$$

where

$$
\overline{q}^C=\frac{q^Ca^4}{Eh^4} \qquad k=\frac{a^2}{Rh} \qquad \zeta=\frac{W}{h} \tag{A.26}
$$

In this case, we have the nonlinear problem of deflection of a thin panel accompanied by an appearance of membrane forces.

The determined dimensionless deflections ζ for $k=0$ (i.e., for the plate) for the assumed value of the transverse load from equation (A.25), within the first order of approximation, are 3.5% less than the exact solution for the plate (Kolakowski and Jankowski, 2021).

Kirchhoff's substitutive transverse forces (A.16), i.e., the bending components of transverse forces, after considering (A.20), are expressed with the dependencies

$$
\begin{aligned}
\widehat{Q}_x^C &= M_{x,x}^C+2M_{xy,y}^C=2DW\Big(\frac{\pi}{a}\Big)^3\Big(\sin\frac{2\pi x}{a}-(3-\nu)\sin\frac{2\pi x}{a}\cos\frac{2\pi y}{a}\Big)\\
\widehat{Q}_y^C &= M_{y,y}^C+2M_{xy,x}^C=2DW\Big(\frac{\pi}{a}\Big)^3\Big(\sin\frac{2\pi y}{a}-(3-\nu)\cos\frac{2\pi x}{a}\sin\frac{2\pi y}{a}\Big)
\end{aligned}
\tag{A.27}
$$

As can be easily seen in (A.27), the bending components are linearly dependent on the deflection W.

Membrane components (A.17), after consideration (A.20) and (A.23), are of the form

$$\begin{aligned}
\overline{Q}_x^C &= N_x w_{,x} + N_{xy} w_{,y} = -EW^3 h\Big(\frac{\pi}{a}\Big)^3\Big[\Big(\frac{1}{8}\cos\frac{2\pi y}{a} - \frac{1}{32}\cos\frac{4\pi y}{a} + \frac{1}{200}\cos\frac{4\pi x}{a}\cos\frac{2\pi y}{a} \\
&+ \frac{1}{50}\cos\frac{2\pi x}{a}\cos\frac{4\pi y}{a} - \frac{1}{16}\cos\frac{2\pi x}{a}\cos\frac{2\pi y}{a}\Big)\sin\frac{2\pi x}{a}\Big(\frac{1}{2} - \frac{1}{2}\cos\frac{2\pi y}{a}\Big) \\
&+ \Big(\frac{1}{100}\sin\frac{4\pi x}{a}\sin\frac{2\pi y}{a} + \frac{1}{100}\sin\frac{2\pi x}{a}\sin\frac{4\pi y}{a} \\
&- \frac{1}{16}\sin\frac{2\pi x}{a}\sin\frac{2\pi y}{a}\Big)\Big(\frac{1}{2} - \frac{1}{2}\cos\frac{2\pi x}{a}\Big)\sin\frac{2\pi y}{a}\Big] \\
&- \frac{EW^2 h}{16R}\frac{\pi}{a}\cos\frac{2\pi x}{a}\cos\frac{2\pi y}{a}\sin\frac{2\pi x}{a}\Big(\frac{1}{2} - \frac{1}{2}\cos\frac{2\pi y}{a}\Big) \\
&+ \frac{EW^2 h}{16R}\frac{\pi}{a}\sin\frac{2\pi x}{a}\sin\frac{2\pi y}{a}\Big(\frac{1}{2} - \frac{1}{2}\cos\frac{2\pi x}{a}\Big)\sin\frac{2\pi y}{a} \qquad \text{(A.28)} \\
\overline{Q}_y^C &= N_y w_{,y} + N_{xy} w_{,x} = -EW^3 h\Big(\frac{\pi}{a}\Big)^3\Big[\Big(\frac{1}{8}\cos\frac{2\pi x}{a} - \frac{1}{32}\cos\frac{4\pi x}{a} + \frac{1}{50}\cos\frac{4\pi x}{a}\cos\frac{2\pi y}{a} \\
&+ \frac{1}{200}\cos\frac{4\pi y}{a} - \frac{1}{16}\cos\frac{2\pi x}{a}\cos\frac{2\pi y}{a}\Big)\Big(\frac{1}{2} - \frac{1}{2}\cos\frac{2\pi x}{a}\Big)\sin\frac{2\pi y}{a} + \Big(\frac{1}{100}\sin\frac{4\pi x}{a}\sin\frac{2\pi y}{a} \\
&+ \frac{1}{100}\sin\frac{2\pi x}{a}\sin\frac{4\pi y}{a} - \frac{1}{16}\sin\frac{2\pi x}{a}\sin\frac{2\pi y}{a}\Big)\sin\frac{2\pi x}{a}\Big(\frac{1}{2} - \frac{1}{2}\cos\frac{2\pi y}{a}\Big)\Big] \\
&+ \frac{EW^2 h}{R}\frac{\pi}{a}\Big(-\frac{1}{16}\cos\frac{2\pi x}{a}\cos\frac{2\pi y}{a} + \frac{1}{4}\cos\frac{2\pi x}{a}\Big)\Big(\frac{1}{2} - \frac{1}{2}\cos\frac{2\pi x}{a}\Big)\sin\frac{2\pi y}{a} \\
&+ \frac{EW^2 h}{16R}\frac{\pi}{a}\sin\frac{2\pi x}{a}\sin\frac{2\pi y}{a}\sin\frac{2\pi x}{a}\Big(\frac{1}{2} - \frac{1}{2}\cos\frac{2\pi y}{a}\Big)
\end{aligned}$$

Membrane components (A.28) are nonlinearly dependent on the deflection W or, more precisely, they depend on the third power of W. The total components of transverse forces, i.e., Kirchhoff's total substitutive forces, are expressed in formulas (A.18).

.0.2. A2.3. Solution to the nonlinear stability problem for the FSDT

For the FSDT, a solution of the system of the last three equations (A.9) is foreseen as (A.20) with respect to the variable w and for the variables ψ_x, ψ_y in the form

$$\psi_x = \Psi_x^F \sin\frac{2\pi x}{a}\sin^2\frac{\pi y}{a} \qquad \psi_y = \Psi_y^F \sin^2\frac{\pi x}{a}\sin\frac{2\pi y}{a} \qquad \text{(A.29)}$$

After substituting variables (A.20), (A.23) and (A.29), the following dependencies are obtained

$$\Psi_x^F = \Psi_y^F = W\alpha\Big(\frac{\pi}{a}\Big)^2 \qquad \text{(A.30)}$$

and

$$\frac{533\pi^4}{3200}\zeta^3 + \frac{2\pi^4}{3(1-\nu^2)}\alpha\zeta - \frac{15\pi^2}{64}k\zeta^2 + \frac{9}{64}k^2\zeta - \overline{q}^F = 0 \qquad \text{(A.31)}$$

where

$$\overline{q}^F = \frac{q^F a^4}{Eh^4} \qquad \alpha = \frac{1}{1+\eta} \qquad \eta = \frac{2\pi^2}{3(1-\nu)K^2}\Big(\frac{h}{a}\Big)^2 \qquad \text{(A.32)}$$

The bending components of transverse forces according to (A.10) are

$$\begin{aligned}
\widehat{Q}_x^F &= M_{x,x}^F + M_{xy,y}^F = 2DW\Big(\frac{\pi}{a}\Big)^3\Big(\sin\frac{2\pi x}{a} - 2\sin\frac{2\pi x}{a}\cos\frac{2\pi y}{a}\Big)\alpha \\
\widehat{Q}_y^F &= M_{y,y}^F + M_{xy,x}^F = 2DW\Big(\frac{\pi}{a}\Big)^3\Big(\sin\frac{2\pi y}{a} - 2\cos\frac{2\pi x}{a}\sin\frac{2\pi y}{a}\Big)\alpha
\end{aligned} \qquad \text{(A.33)}$$

As for the CST, the bending components are linearly dependent on the deflection W. Comparing (A.33) to (A.27), it can be easily seen that there is a factor of 2 in the FSDT, and a factor $(3-\nu)$ for the CST at the second term in the parentheses.

The membrane components of transverse forces (A.11) for the FSDT have the same form as for the CST (A.17), i.e.

$$\overline{Q}_x^F = \overline{Q}_x^C \qquad \overline{Q}_y^F = \overline{Q}_y^C \tag{A.34}$$

whereas the components of the total transverse forces are expressed by (A.12), respectively.

Funding
This research received no external funding.

References

1. Bathe K.J., 1996, *Finite Element Procedures*, Prentice-Hall International, Inc.
2. Cai L., Rong T., Chen D., 2002, Generalized mixed variational methods for Reissner plate and its applications, *Computational Mechanics*, **30**, 29-37
3. Cen S., Shang Y., 2015, Developments of Mindlin-Reissner plate elements, *Mathematical Problems in Engineering*, ID 456740
4. Endo M., Kimura N., 2007, An alternative formulation of the boundary value problem for the Timoshenko beam and Mindlin plate, *Journal of Sound and Vibration*, **301**, 355-373
5. Kim S.E., Thai H-T., Lee J., 2009, A two variable refined plate theory for laminated composite plates, *Composite Structures*, **89**, 197-205
6. Kołakowski Z., Jankowski J., 2020, Effect of membrane components of transverse forces on magnitudes of total transverse forces in the nonlinear stability of plate structures, *Materials*, **13**, 22, 5262
7. Kolakowski Z., Jankowski J., 2021, Some inconsistencies in the nonlinear buckling plate theories – FSDT, S-FSDT, HSDT, *Materials*, **14**, 9, 2154
8. Mindlin R.D., 1951, Influence of rotatory inertia and shear on flexural motions of isotropic, elastic plates, *ASME Journal of Applied Mechanics*, **18**, 1, 31-38
9. Park M., Choi D.-H., 2018, A two-variable first-order shear deformation theory considering in-plane rotation for bending, buckling and free vibration analyses of isotropic plates, *Applied Mathematical Modelling*, **61**, 49-71
10. Reddy J.N., 2004, *Mechanics of Laminated Composite Plates and Shells: Theory and Analysis*, 2nd ed., CRC Press, Boca Raton, FL
11. Reddy J.N., 2011, A general nonlinear third-order theory of functionally graded plates, *International Journal of Aerospace and Lightweight Structures*, **1**, 1, 1-21
12. Reissner E., 1944, On the theory of bending of elastic plates, *Journal of Mathematics and Physics*, **23**, 184-191
13. Reissner E., 1945, The effect of transverse shear deformation on the bending of elastic plates, *ASME Journal of Applied Mechanics*, **12**, 2, A69-A77
14. Shimpi R.P., Patel H.G., 2006, A two-variable refined plate theory for orthotropic plate analysis, *International Journal of Solids and Structures*, **43**, 6783-6799
15. Shimpi R.P., Shetty R.A., Guha A., 2017, A single variable refined theory for free vibrations of a plate using inertia related terms in displacements, *European Journal of Mechanics A/Solids*, **65**, 136-148

16. Taylor M.W., Vasiliev V.V., Dillard D.A., 1997, On the problem of shear-locking in finite elements based on shear deformable plate theory, *International Journal of Solids and Structures*, **34**, 7, 859-875

17. Vasiliev V.V., 2000, Modern conceptions of plate theory, *Composite Structures*, **48**, 39-48

18. Vasiliev V.V., Lurie S.A., 1992, On refined theories of beams, plates, and shells, *Journal of Composite Materials*, **26**, 4, 546-557

19. Volmir A.S., 1967, *Stability of Deformable Systems* (in Russian), Science Publishing House, Moscow, 984

20. Volmir A.S., 1972, *Nonlinear Dynamics of Plates and Shells* (in Russian), Science Publishing House, Moscow, 432

Manuscript received May 17, 2022; accepted for print July 24, 2022